Acta Biomaterialia 7 (2011) 1184–1191

Contents lists available at ScienceDirect

Acta Biomaterialia

journal homepage: www.elsevier.com/locate/actabiomat

Dynamic mechanical analysis and biomineralization of hyaluronan–polyethylene copolymers for potential use in osteochondral defect repair

Rachael A. Oldinski [a], Timothy T. Ruckh [b], Mark P. Staiger [c], Ketul C. Popat [a,b], Susan P. James [a,b,*]

[a] Department of Mechanical Engineering, Campus Delivery 1374, Colorado State University, Fort Collins, CO 80523-1374, USA
[b] School of Biomedical Engineering, Campus Delivery 1376, Colorado State University, Fort Collins, CO 80523-1374, USA
[c] Department of Mechanical Engineering, University of Canterbury, Private Bag 4800, Christchurch 8020, New Zealand

ARTICLE INFO

Article history:
Received 17 May 2010
Received in revised form 10 November 2010
Accepted 17 November 2010
Available online 21 November 2010

Keywords:
Hyaluronan
Polyethylene
Dynamic unconfined compression
Bone marrow stromal cell
Articular cartilage

ABSTRACT

Treatment options for damaged articular cartilage are limited due to its lack of vasculature and its unique viscoelastic properties. This study was the first to fabricate a hyaluronan (HA)–polyethylene copolymer for potential use in the replacement of articular cartilage and repair of osteochondral defects. Amphiphilic graft copolymers consisting of HA and high-density polyethylene (HA–co-HDPE) were fabricated with 10, 28 and 50 wt.% HA. Dynamic mechanical analysis was used to assess the effect of varying constituent weight ratios on the viscoelastic properties of HA–co-HDPE materials. The storage moduli of HA–co-HDPE copolymers ranged from 2.4 to 15.0 MPa at physiological loading frequencies. The viscoelastic properties of the HA–co-HDPE materials were significantly affected by varying the wt.% of HA and/or crosslinking of the HA constituent. Cytotoxicity and the ability of the materials to support mineralization were evaluated in the presence of bone marrow stromal cells. HA–co-HDPE materials were non-cytotoxic, and calcium and phosphorus were present on the surface of the HA–co-HDPE materials 2 weeks after osteogenic differentiation of the bone marrow stromal cells. This study is the first to measure the viscoelastic properties and osseocompatibility of HA–co-HDPE for potential use in orthopedic applications.

1. Introduction

Articular cartilage lacks the vasculature to provide the cells and nutrients necessary for healing, and has a limited capacity for self-regeneration after injury or disease. When articular cartilage becomes damaged, the tissue structure and properties are altered, eventually leading to joint pain, which affects millions of people world-wide. Treatment options for partial or full-thickness articular cartilage lesions (i.e. osteochondral defects) involve the removal of a small area of damaged articular cartilage, exposing subchondral bone. Subsequent surgical techniques may include abrasion arthroplasty, subchondral drilling, autologous osteochondral grafting, periosteal–perichondral grafting and chondrocyte transplantation [1]. Autograft and allograft full-thickness osteochondral plugs (containing both cartilage and subchondral bone) are harvested from non-load-bearing areas of healthy tissue and implanted into the defect on the articulating joint surface. These latter techniques result in pain and morbidity at the donor site and subsequent damage to adjacent tissue. Moreover, postoperative recovery requires a period during which the repair is prevented from bearing weight.

Hyaluronan (HA) is a biologically active glycosaminoglycan found ubiquitously throughout the body, including the extracellular matrix of articular cartilage [2], and has a long-standing history of use in numerous medical applications, including dermatology, ophthalmology, otolaryngology, wound repair, drug delivery, tissue engineering and osteochondral defect repair [3–7]. The use of HA is advantageous because it is biocompatible and participates in numerous biological functions [8,9]. HA–cell surface receptor interactions activate a series of intracellular signaling pathways and participate in the regulation of cell migration [10] and proliferation [11], and the differentiation of mesenchymal stem cells [12]. CD44–HA interactions are essential for maintaining normal cartilage homeostasis, e.g. modulating cartilage metabolism by linking cells with their extracellular environment [13,14]. HA has the capacity to modify osteoblast behavior and plays an important role in both the early and later stages of bone formation; in particular, high molecular weight HA is osteoinductive in vivo [14] and significantly increases bone mineralization [15].

In the hydrated state, HA has the ability to bear compressive forces and contributes to the hydrodynamic properties of articular cartilage. The dynamic, unconfined equilibrium modulus of healthy articular cartilage has been reported to be 4–8 MPa at physiological loading conditions [16,17]. Under compression, articular cartilage behaves like a poroelastic material, in which its response to compressive loads is frequency and strain dependent.

* Corresponding author at: Department of Mechanical Engineering, College of Engineering, Colorado State University, Campus Delivery 1374, Fort Collins, CO 80523-1374, USA. Tel.: +1 970 491 2842; fax: +1 970 491 3827.
E-mail address: sjames@engr.colostate.edu (S.P. James).

1742-7061/$ - see front matter © 2010 Published by Elsevier Ltd. on behalf of Acta Materialia Inc.
doi:10.1016/j.actbio.2010.11.019

These properties are governed by the interrelationship between the solid extracellular matrix constituents, interstitial fluid flow [18], intact collagen network and a high concentration of the HA-containing proteoglycan aggrecans [14]. However, HA, either in its native state or as a physically crosslinked gel, is too compliant for load-bearing applications such as articular cartilage replacement [19].

Various chemical crosslinking strategies aimed at improving the mechanical properties of HA to better mimic those of articular cartilage have been explored. The HYAFF® 11 sponge is made from a linear HA derivative in which the carboxyl groups are esterified with benzyl groups, whereas the ACP™ sponges are crosslinked derivatives of HA in which the carboxylic acid groups are linked via an ester bond between hydroxyl groups on adjacent HA chains [2]. Both HA-derived hydrogels were found to be biocompatible and integrate with bone and cartilage [4]; however, under static unconfined compression the Young's moduli of HYAFF® 11 and ACP™ sponges were 42.1 and 7.6–8.2 kPa, respectively, making them much more compliant than articular cartilage. The modulus mismatch between articular cartilage and tissue engineering constructs, such as HYAFF® 11 and ACP™, may harm surrounding and opposing tissue by redistributing stresses in vivo, potentially contributing to the initiation and development of post-traumatic osteoarthritis. Hence, there is a need to develop stiffer HA-based hydrogels with properties similar to articular cartilage to restore function to a joint immediately after osteochondral defect repair.

Synthetic materials such as non-degradable poly(vinyl alcohol) have been developed as permanent osteochondral plugs rather than scaffolds for cartilage regrowth to overcome the limitations of conventional techniques [20–22]. Poly(vinyl alcohol) and titanium fiber mesh composite implants exhibited strong attachment to canine femoral bone 12 months postoperatively [23,24]. However, the shear properties of the construct were insufficient due in part to differences in the elastic moduli of the poly(vinyl alcohol) hydrogel and the titanium. In addition, poly(vinyl alcohol) is not bioactive, and thus does not promote cartilage repair or bone integration; long-term success therefore depends upon the mechanical integrity of the poly(vinyl alcohol) hydrogel/titanium fiber mesh implant as well as the integration of the implant with host tissues. Insufficient mineralization will fail to stabilize the implant and result in additional articular cartilage damage due to micromotion. Thus, a permanent material for the replacement of damaged osteochondral tissue has yet to be developed which mimics the viscoelastic properties of articular cartilage and provides a means by which to stabilize the implant, such as osseointegration.

The various hydrogels designed for the treatment of osteochondral defects do not provide viscoelastic properties comparable to those of articular cartilage. Tissue engineering scaffolds may also result in fibrocartilage or mineralized cartilage, which are undesired, and bioinert synthetic polymers integrate poorly with surrounding tissues. Biomaterials designed for osteochondral defect repair must promote the health of adjoining tissues and provide mechanical stability. The purpose of this study was to synthesize and evaluate an HA–high-density polyethylene graft copolymer (HA–co-HDPE) for the repair of osteochondral defects. Our long-term goal is to create a permanent biomaterial which can replace articular cartilage and match its viscoelastic properties while supporting mineralization for bone integration and stabilization of the implant. It was proposed that the copolymerization with polyethylene would stiffen HA and that the viscoelastic properties of HA–co-HDPE could be tailored as an articular cartilage replacement by modifying copolymer composition (i.e. HA content and covalent crosslinking). Furthermore, it was anticipated that the HA–co-HDPE would be non-cytotoxic and support mineralization due to the incorporation of HA.

2. Materials and methods

2.1. HA–co-HDPE synthesis and compression molding

Methods for producing an ammonium salt-complexed derivative of HA have previously been reported [25,26]. Briefly, HA (Genzyme, 650 kDa) and hexadecyltrimethylammonium bromide (CTAB) solutions were mixed together at room temperature to form the precipitate, HA–CTA. A 0.1% (w/v) maleic anhydride graft HDPE (MA–g-HDPE) (Solvay Plastics, 15 kDa, 3 wt.% MA) solution was refluxed in xylenes then added to a 0.5% (w/v) HA–CTA solution in dimethyl sulfoxide. The solution was vigorously mixed for 12 h at 110 °C then vacuum dried at 50 °C for 72 h. The reaction products were added to a 0.2 M NaCl solution to remove the CTA^+ salt. The HA–co-HDPE product was washed with ethyl alcohol, resuspended in deionized water, and vacuum dried at room temperature. HA–co-HDPE was fabricated with theoretical weight ratios (based on reactant stoichiometry) of 10%, 28% and 50% (10%-HA, 28%-HA and 50%-HA).

Prior to melt processing, the melting temperature (T_m) of HA–co-HDPE was determined by differential scanning calorimetry under nitrogen (TA Instruments DSC 2920) according to ASTM D3418 (samples were heated from room temperature to 180 °C at a rate of 10 °C min^{-1}). The average T_m of the different HA–co-HDPE formulations was found to be approximately 100 °C. Thus, HA–co-HDPE powder was compression molded at 110 °C under 8 MPa for 10 min in an inert atmosphere. The HA portion of the compression-molded graft copolymer was chemically crosslinked after compression molding (select samples) via poly(hexamethylene diisocyanate) [26], forming chemically crosslinked HA–co-HDPE with 10, 28 and 50 wt.% HA (xlinked 10%-HA, xlinked 28%-HA, xlinked 50%-HA).

2.2. Dynamic mechanical analysis

Cylindrical acellular HA–co-HDPE samples (10%-HA, xlinked 10%-HA, 50%-HA, xlinked 50%-HA) and MA–g-HDPE control, with nominal heights of 2 mm and diameters of 4 mm, were soaked in phosphate-buffered saline (PBS) at room temperature for 12 h prior to testing ($n = 3$). Pure HA was not tested since it could only be produced as a thin film after chemical crosslinking. An initial quasi-static compression test was performed to determine the upper strain limit of the linear viscoelastic range, and all samples were tested using strains below this limit. Samples were preconditioned in PBS for 20–25 min using the same loading profile used in testing: samples were preloaded to 300 mN (23.87 kPa) and dynamically compressed in load control with 10 μm strain amplitude (0.5% strain). The storage (E') and loss (E'') moduli were measured in unconfined compression under this load and strain amplitude (Perkin Elmer Diamond DMA) at frequencies of 0.01, 0.1, 1 and 10 Hz while the samples were fully immersed in 37 °C PBS solution.

2.3. Bone marrow stromal cell isolation and culture

Compression-molded HA–co-HDPE with 10 wt.% HA, chemically crosslinked HA-co-HPDE with 10 wt.% HA (10%-HA, xlinked 10%-HA), and tissue culture polystyrene controls were adhered to the bottom of 24-well tissue culture plates with medical-grade adhesive (Nexaband®, Abbot Laboratories) for the bone marrow stromal cell (BMSC) study. Samples were disinfected with 70% ethanol, rinsed with PBS, exposed to UV in a laminar flow hood for 10 min, and soaked in medium 2 h prior to seeding with BMSCs. Studies were performed in triplicate for all samples. 10%-HA and xlinked 10%-HA samples were chosen for the in vitro study because

they were previously shown to have less of an impact on ALP production, compared to the 28%-HA and 50%-HA groups, when cultured with a human osteoblast cell line [27], and thus provided a "worse-case" scenario for osseogenic activity.

BMSCs were isolated from Wistar rats (*Rattus norvegicus*) supplied by Harlan Sprague Dawley Inc. Limbs were aseptically removed from recently killed animals. Soft tissue was removed and the bones were briefly stored in cold PBS before isolating cells. The metaphyseal ends of the bones were removed to expose the bone marrow cavity. In a 50 ml conical tube, marrow was repeatedly flushed with culture medium (α-MEM with 10% fetal bovine serum and 1% penicillin/streptomycin) using 10 ml syringes with 18 and 25 gauge needles. Medium containing cells and debris was filtered with a 70 μm nylon filter into a clean tube. Cells were seeded on samples in a 24-well plate at a density of 1×10^6 cells well^{-1}. Cells were cultured in the same medium as described above. Cultures were incubated at 37 °C and 5% CO_2 for the duration of the study. Half of the medium was changed on day 4. On day 7, all the medium was replaced with an osteogenic differentiation medium consisting of α-MEM supplemented with 10% fetal bovine serum, 1% penicillin/streptomycin, dexamethasone (10^{-8} M), ascorbic acid (50 μg ml^{-1}) and β-glycerolphosphate (8 mM). The medium was changed every 2 or 3 days with osteogenic medium up to 2 weeks. The duration of the entire experiment was 21 days.

2.4. BMSC adhesion and proliferation

Cell responses to the hydrogels were investigated through cell adhesion, viability (mitochondrial activity) and morphology. Cell viability was measured after 1 and 4 days of culture (log phase growth) using a commercially available MTT assay kit (Sigma). Adhered cells were incubated at 37 °C for 3 h in a (3-[4,5-dimethylthiazol-2-yl]-2,5-diphenyl tetrazolium bromide (MTT) solution. Mitochondrial dehydrogenases of viable cells cleave the tetrazolium ring, yielding purple formazan crystals. Formazan crystals were then dissolved in the MTT solvent with 10 vol.% Triton-X. The optical density (OD) of the solvent is proportional to the mitochondrial activity of the cells on the surface. OD was measured at 570 nm using a spectrophotometer (FLUOstar Omega, BMG Labtech, Durham, NC). Background absorbance at 690 nm was subtracted from the measured absorbance. Blank samples with no cells were used to normalize the data.

Cell adhesion was investigated using a commercially available live/dead assay. Calcein–AM can penetrate live cell membranes, where the AM is cleaved and the resulting calcein molecule fluoresces green (excitation/emission ~495 nm/~515 nm). The cells were incubated in 2 μM of calcein–AM solution in PBS for 45 min and were imaged with a fluorescence microscope (Zeiss) with appropriate filters. Ethidium homodimer-1 enters cells with damaged membranes and undergoes a 40-fold enhancement of fluorescence upon binding to nucleic acids, thereby producing a bright red fluorescence in dead cells (excitation/emission ~495 nm/~635 nm).

2.5. BMSC differentiation

Cellular response to the hydrogels was investigated 1 and 2 weeks after providing the cells with osteogenic differentiation medium. Intracellular protein content was used to look at cellular functionality during differentiation and to normalize the calcium assay data. Calcium and phosphate deposition on the hydrogels was used to assess the osseoconductive properties. Hydrogels and control substrates were removed from the culture media and rinsed twice in PBS prior to analysis.

To determine the total protein content, the adhered cells were lysed with Cell Lytic™ solution (Sigma) for 1 h. The total protein content of the lysate was measured using a commercially available protein assay and the absorbance of the solution was measured using a plate reader at a wavelength of 570 nm. The absorbance was then converted to protein content using an albumin standard curve to determine the amount of intracellular protein.

In order to stain the hydrogels and controls for phosphate, they were rinsed twice with cacodylate buffer and then immersed in 4% paraformaldehyde (w/v) in cacodylate buffer for 10 min. They were then rinsed with deionized water, and then a solution of silver nitrate in deionized water was added for 20 min, allowing the phosphate and silver nitrate to react to form a brown precipitate. The reaction was stopped by rinsing three times with de-ionized water. The hydrogels were dried in a desiccator and digital images of stained surfaces were captured using a Canon PowerShot SD1000.

In order to stain the hydrogels and controls for deposited calcium, they were rinsed twice in cold (4 °C) Ringer's solution. They were then immersed in cold 4% paraformaldehyde (w/v) in PBS solution for 10 min, rinsed in cold deionized water, and submerged in cold alizarin red solution (2 wt.%) in sodium hydroxide for 10 min. The hydrogels were rinsed three times with cold deionized water and allowed to dry in a desiccator. Calcium forms an alizarin red S–calcium complex via a chelation process, and the end product is birefringent. Digital images of stained surfaces were captured using a Canon PowerShot SD1000.

The amount of calcium deposited on materials was quantified using a commercially available colorimetric kit (Bioassay Systems QuantiChrom). Hydrogels and control substrates were removed from culture wells, rinsed twice with PBS and incubated in 6 M HCl for 2 h at room temperature to release and dissolve the calcium on the surface. The amount of calcium deposition was measured using the *o*-cresolphthalein complexone method which forms a colored complex that absorbs at 570 nm [28–30]. The color intensity was measured with a spectrophotometer and calibrated by a standard solution of known concentration.

Mineralization on the hydrogels was also investigated using field emission scanning electron microscopy (SEM) (JEOL JSM-6500F). The hydrogels were gently removed from the culture media and immersed in PBS for 5 min to remove unadhered cells and proteins. The cells were then fixed in a fixing solution (3% glutaraldehyde with 0.1 M sucrose and 0.1 M sodium cacodylate in deionized water) for 45 min, rinsed in a buffer solution (fixing solution without glutaraldehyde), and then dehydrated in increasing concentrations of ethanol (30%, 50%, 70%, 90% and 100%) for 10 min each. After dehydration the hydrogels were immersed in hexamethyldisilazane (HDMS) for 10 min and then air-dried. The hydrogels were stored in a desiccator until further characterization. They were then sputter-coated with 10 nm of gold and imaged by SEM. Samples prepared for SEM were also examined for surface elemental composition using an energy-dispersive X-ray spectroscopy (EDX) probe (Thermo Electron, Noran system) attached to the JEOL JSM 6500F microscope. EDX was used to detect mineralization (calcium and phosphorus) on the samples. Instrument aperture and probe current were adjusted to give a dead time of between 15% and 20%. Surfaces were analyzed for 5 min at 5–15 kV and a magnification of 100–5000× to provide a complete profile of the different elements present. Spatial element mapping was performed by grouping pixels with similar atomic spectra.

2.6. Statistical analysis

All the substrates were cultured and assayed in triplicate at each time point specified. All the studies were conducted in triplicate using different animals as the BMSC source for each study. The data was pooled from the studies using different cell sources ($n = 9$). All the statistics are presented here as mean ± standard deviation. A two-tailed, unpaired *t*-test was performed to determine the statistical significance, defined as a *P*-value less than 0.05.

3. Results

3.1. Dynamic mechanical analysis

Unconfined dynamic compression testing was performed to determine the storage modulus, E', loss modulus, E'', and tan δ of the various HA–co-HDPE formulations; the data is presented in Fig. 1. Collectively, the E' of the various copolymer compositions were observed to range from 2.4 to 4.4 MPa at 0.01 Hz, 3.3 to 4.24 MPa at 0.1 Hz, 4.9 to 10.6 MPa at 1 Hz, and 6.7 to 15.0 MPa at 10 Hz. The E' for the MA–g-HDPE control, which was an order of magnitude higher (significantly higher) compared to the HA–co-HDPE samples, ranged from 35.5 to 76.0 MPa at 0.01 and 10 Hz, respectively. For all HA–co-HDPE samples, E' increased as loading frequency increased. The xlinked 28%-HA and 28%-HA groups were the stiffest at all loading frequencies, while the xlinked 10%-HA group was the most compliant. At all loading frequencies, the xlinked 28%-HA group had a significantly higher ($P < 0.05$) storage modulus compared to the xlinked 10%-HA group.

The MA–g-HDPE control exhibited significantly higher E'' compared to all of the HA–co-HDPE samples. At 0.1 Hz, the E'' of the MA–g-HDPE control peaked, then began to decrease, whereas the E'' of the HA–co-HDPE materials increased with increasing loading frequency. The 28%-HA and xlinked 28%-HA groups exhibited higher E'' values compared the other HA–co-HDPE groups. At 0.01 Hz, the xlinked 28%-HA group had a significantly higher ($P < 0.05$) loss modulus compared to the xlinked 10%-HA, 10%-HA and 50%-HA groups; the 28%-HA also had a significantly higher loss modulus compared to the xlinked 10%-HA group. At 0.1 Hz, the xlinked 28%-HA had a significantly higher loss modulus compared to the 50%-HA group ($P < 0.04$). At 1.0 and 10 Hz, the xlinked 28%-HA group had a significantly higher loss modulus compared to the xlinked 10%-HA group ($P < 0.04$).

The tan δ data reflects the ratio of the trends in the E'' to the trends in the E' data. The HA–co-HDPE samples exhibited higher tan δ values than the MA–g-HDPE control at 0.1, 1.0 and 10 Hz. At 0.01 Hz, the 28%-HA and xlinked 28%-HA groups had significantly higher ($P < 0.02$) tan δ values compared to the 10%-HA, xlinked 10%-HA and 50%-HA groups. At 0.1 Hz, the xlinked 28%-HA group had a significantly higher ($P < 0.01$) tan δ compared to the 10%-HA and 50%-HA groups. At 1.0 Hz, the 28%-HA and xlinked 28%-HA groups had significantly higher ($P < 0.03$) tan δ values compared to the 10%-HA group. At 10 Hz, the 50%-HA group had a significantly higher ($P < 0.05$) tan δ compared to the 10%-HA, xlinked 10%-HA and xlinked 28%-HA groups. The xlinked 28%-HA was significantly higher ($P < 0.05$) compared to the 10%-HA, xlinked 10%-HA and 28%-HA groups.

3.2. BMSC adhesion and proliferation

BMSCs were viable on both HA–co-HDPE samples, 10%-HA and xlinked 10%-HA, after 4 days of initial culture. The MTT absorbance values for the 10%-HA and xlinked 10%-HA samples were not significantly different at either time point; the results of the MTT assay after 1 and 4 days of culture are shown in Fig. 2. Cell adhesion was investigated using a commercially available live/dead assay after 4 and 7 days of culture. Representative images of live (stained green) and dead (stained red) cells on the surface of 10%-HA and xlinked 10%-HA samples are shown in Fig. 3; images were taken at 10× magnification. A significantly higher number of live cells are present on both materials after 4 and 7 days of culture compared to dead cells.

3.3. BMSC differentiation

To investigate the ability of these materials to promote mineralization and osseointegration, cellular production of calcium phosphate was examined after osteogenic differentiation of the BMSCs using a calcium assay, aliziran red and von Kossa staining,

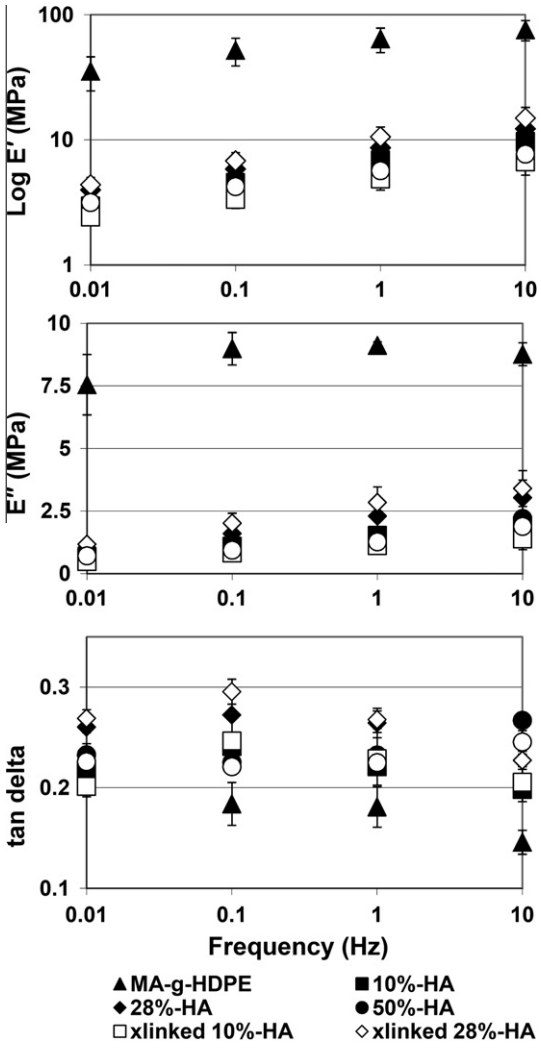

Fig. 1. Storage moduli (E'), loss moduli (E'') and tan δ (average ± standard deviation) of HA–co-HDPE samples and a MA–g-HDPE control tested in dynamic unconfined compression in PBS at 37 °C ($n = 3$).

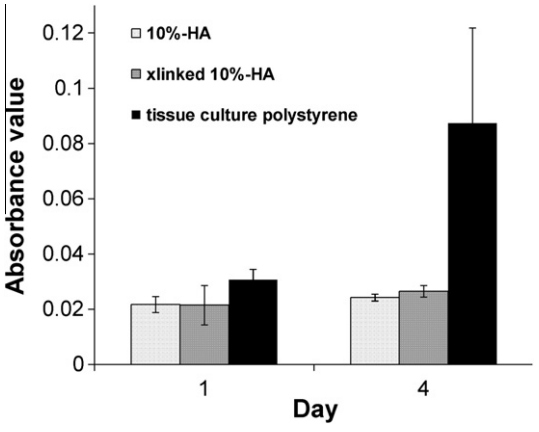

Fig. 2. MTT cytotoxicity assay results (average ± standard deviation) for HA–co-HDPE samples and a tissue culture polystyrene control after 1 and 4 days of initial culture.

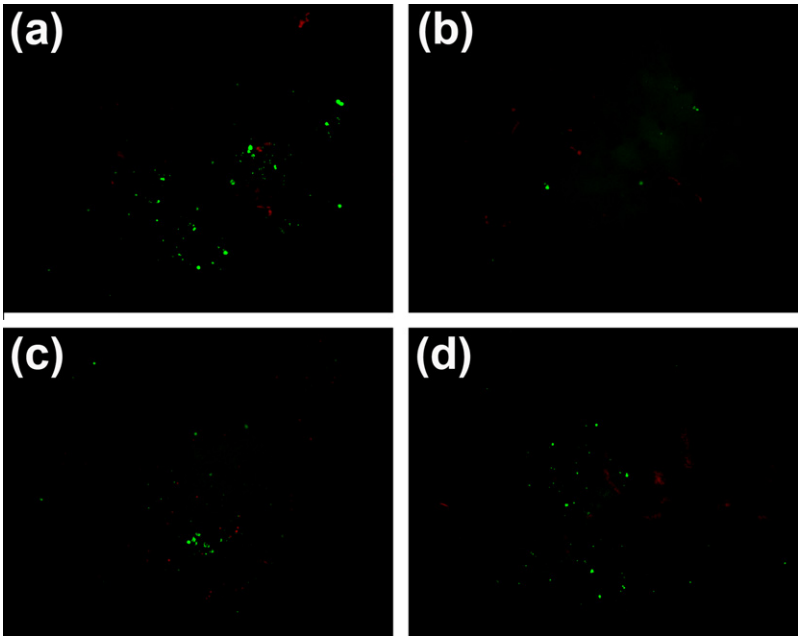

Fig. 3. Fluorescent microscopy images taken at 10× magnification of BMSC-seeded hydrogels after 4 and 7 days of culture. Live cells = green; dead cells = red.

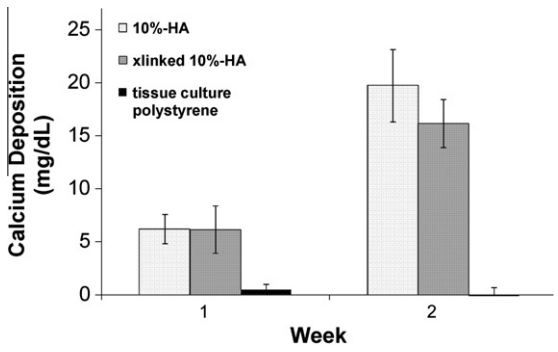

Fig. 4. Calcium assay results (average ± standard deviation) for bone marrow stromal cell seeded HA–co-HDPE samples and a tissue culture polystyrene control 1 and 2 weeks after differentiation ($n = 3$).

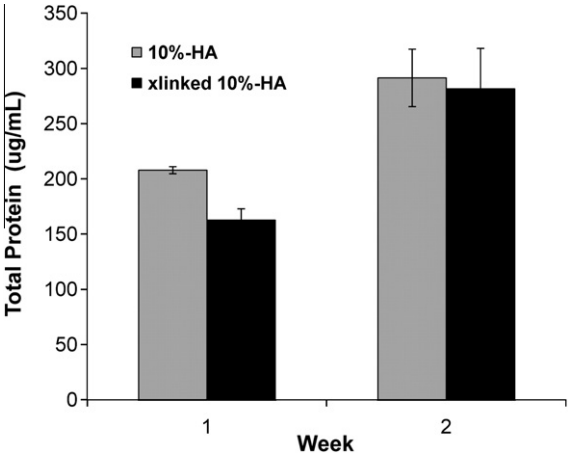

Fig. 5. Total protein content measured using BCA assay (average ± standard deviation) for HA–co-HDPE samples after 1 and 2 weeks of differentiation.

and SEM and EDS. The amounts of calcium measured for the 10%-HA and xlinked 10%-HA materials were significantly higher ($P < 0.05$) compared to the tissue culture polystyrene control for all time points (shown in Fig. 4); the 10%-HA and xlinked 10%-HA materials were not significantly different from each other. The results of the BCA assay after 1 and 2 weeks of culture are shown in Fig. 5.

Fig. 6 shows digital photographs of the stained surfaces (calcium (red) on top; phosphate (brown) stain on the bottom) 2 weeks after differentiation. The intensity of the stain for both HA scaffolds appeared to have similar intensities at both time points. The von Kossa stains were very dark, indicating a dense presence of phosphates on the surface, while the alizarin calcium stain was less stark but still indicated a dense presence of calcium on the hydrogel surfaces. For both stains, the TCPS control revealed less mineralization. Calcium phosphate minerals in the early form of spherulites or globules were observed after 1 week of differentiation on HA–co-HDPE materials. SEM images after 2 weeks of differentiation of 10%-HA and xlinked 10%-HA samples are shown in Fig. 7, in addition to an EDS elemental compositional map of the HA–co-HDPE surfaces. EDS confirmed the presence of calcium and phosphorus on the hydrogels, suggesting mineralization.

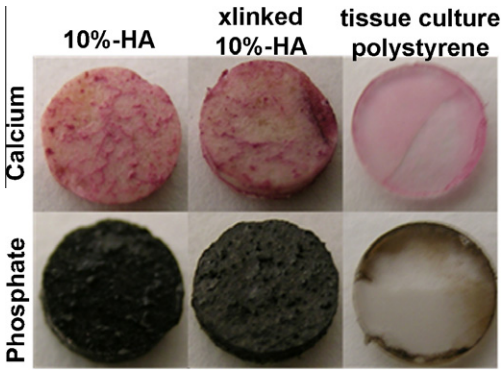

Fig. 6. Images of HA–co-HDPE samples and a tissue culture polystyrene control stained for calcium and phosphate 2 weeks after differentiation.

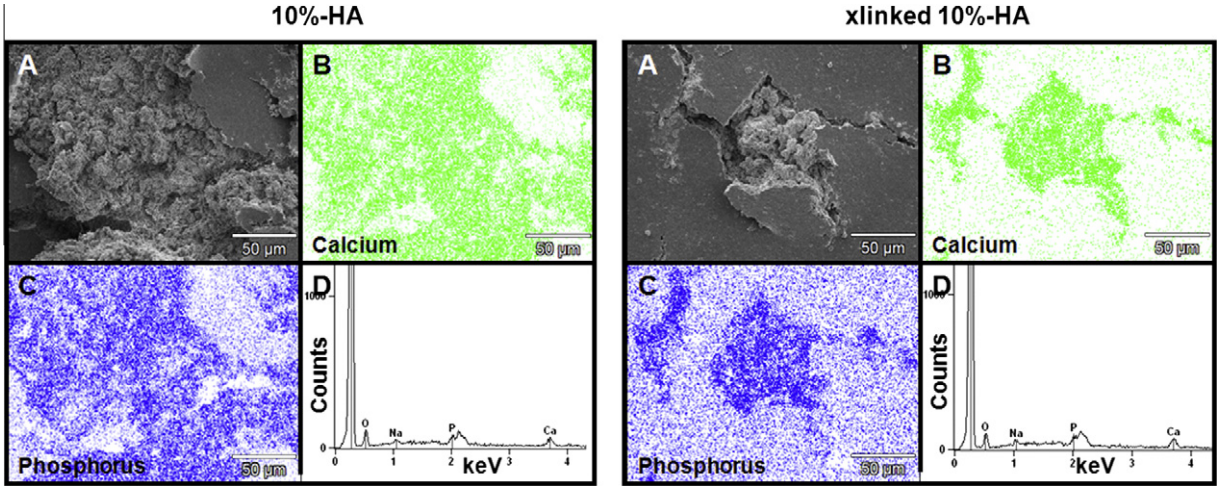

Fig. 7. SEM image (A) and EDS map and spectra (B–D) of HA–co-HDPE samples (10%-HA = left, xlinked 10%-HA = right) 2 weeks after differentiation; calcium and phosphorus were shown to be present. SEM images were taken at 500× magnification.

4. Discussion

This study investigated the viscoelastic properties, cytotoxicity and biomineralization potential of novel HA–co-HDPE materials as permanent implants for the repair of osteochondral defects. HA was incorporated to utilize its viscoelastic and osseoinductive properties, while HDPE was grafted onto HA to improve the material's stiffness compared to HA hydrogels. The individual mechanical properties of HA and HDPE differ significantly from those of articular cartilage, HA being much more compliant and HDPE being much stiffer than articular cartilage [4,18]. The novel HA–co-HDPE materials exhibited mechanical behavior characteristic of healthy articular cartilage, indicating promise as a permanent replacement for cartilage in osteochondral defects. The viscoelastic properties of the HA–co-HDPE materials were dominated by the presence of HDPE; modifying the weight per cent of HA in the HA–co-HDPE did not result in a significant correlation between moduli values and per cent HA. The crystalline domains and tie molecules (e.g. physical crosslinks) within the HDPE increased the stiffness of the HA–co-HDPE materials compared to HA-based hydrogels. The HDPE stiffening of the HA material is akin to the stiffening effect of collagen fibers on the HA-rich extracellular matrix of cartilage. It is also clear that the introduction of HA did significantly alter the mechanical performance of the HDPE, resulting in a much more compliant material. While HDPE has a much higher modulus than the range of moduli reported for cartilage in the literature, the HA–co-HDPE materials tested herein have moduli values closer to those reported for articular cartilage [16,31].

The dynamic modulus of articular cartilage varies depending on the age and species of the animal, location, loading frequency [32] and tissue preparation method. Although a tissue sample control was not used for this study, the parameters of the dynamic mechanical analysis enable us to make comparisons between the properties of the experimental samples and articular cartilage. Loading frequencies of 0.01–10 Hz were used in the current study as they represent physiologically relevant frequencies [33]. The compressive strain amplitude of 0.5% used for the current study is relatively low compared to some testing regimes of 5–20% strain used by other researchers [16]. In addition, lower preloads and compressive strain amplitude were used in this study because all samples had to be tested under the same conditions and these were the highest preload and strain amplitude that the dynamic mechanical analyzer could apply to the relatively stiff MA–g-HDPE control samples. Since the samples in this study and in other studies were all tested within their respective linear elastic ranges, comparisons can be made between the dynamic moduli, which should not be strain amplitude dependent within the linear elastic regions of the respective materials.

At 0.1 Hz, the unconfined dynamic stiffness of articular cartilage has been reported as 4–8 MPa. The storage moduli for the HA–co-HDPE materials were very similar to those of articular cartilage at 0.1 Hz, and ranged from 3.7 to 8.1 MPa (Fig. 1). The storage modulus for the MA–g-HDPE control was 42.9 MPa at 0.1 Hz. Tan δ represents the damping capacity of the material or the ratio of energy dissipated (E'') to energy stored (E'). The HA–co-HDPE samples had higher tan δ values (i.e. more energy dissipation) than the MA–g-HDPE samples. It was expected tan δ would decrease with an increase in loading frequency; this was not seen in all of the materials over the test range. Future work may investigate the HA–co-HDPE behavior under larger strains and directly compare it to cartilage tissue tested under the same conditions.

HA–co-HDPE was developed for use in the permanent replacement (i.e. not as a tissue engineering scaffold) of articular cartilage and repair of osteochondral defects [34]. Since BMSCs are found naturally in vivo, and since articular cartilage replacements are often anchored in place via osseointegration with subchondral bone, their interaction with hydrogels was investigated [35]. BMSCs seeded on crosslinked and non-crosslinked HA–co-HDPE materials did not exhibit cytotoxic effects, assessed using an MTT assay (shown in Fig. 2). Fluorescent images of BMSCs seeded on the HA–co-HDPE materials indicated that more live cells were present than dead ones at both time points (shown in Fig. 3). Live cells were also seen on the tissue culture polystyrene control (images not shown). The cells appear to be round in shape as opposed to spread out on the surface of the HA–co-HDPE hydrogels. It has been reported in the literature that BMSCs cultured on porous hydrogels exhibit a round morphology on the surface of the materials [36] and tend to migrate into the bulk of the material [37]. Therefore, it was theorized that the cells migrated into the material and proliferated rather than remaining on the surface, since few cells were seen on the surface of the materials after 3 weeks of culture [38]. This theory is supported by the increase in calcium content on the HA–co-HDPE materials and the increase in intracellular protein concentration over the culture period of 2 weeks.

The performance and clinical relevance of a biomaterial designed for bone integration relies heavily on its ability to accelerate the cellular production of organic and inorganic extracellular matrix, in order to integrate with surrounding osseous tissue. EDS

analysis was performed on HA–co-HDPE materials before differentiation to demonstrate that no calcium or phosphorus was present on the sample; therefore, mineralization was cell-based as a result of BMSC differentiation to osteoblasts and not due to protein interaction with the HA-containing materials. The SEM images and corresponding EDS maps shown in Fig. 7 demonstrate the ability of the differentiated BMSCs to deposit inorganic matrix compounds on the HA–co-HDPE materials. The surfaces of the HA–co-HDPE materials appeared smoother before differentiation compared to the rough, rocky appearance of the materials after differentiation. The intensity of the calcium and phosphorus deposition on the HA–co-HDPE materials was significantly greater compared to the tissue culture polystyrene control, which is attributed to the bioactive component, HA, and not deposition of some form of calcium phosphate from the medium used for cell culture. This was also true for the calcium assay and was seen on the EDS images from SEM. The mineral morphology is well supported in the literature as evidence of an early phase of biomineralization [37–38].

This study was limited by the absence of an articular cartilage tissue control for the direct mechanical analysis experiments. Properties of articular cartilage reported in the literature cover a broad range; this can be explained by the intrinsic differences in the material properties of tissue from different species, the age of specimen and the location of the specimen in the joint space/body. However, this study does confirm that the HA–co-HDPE material may be tailored to match a range of properties that includes those of cartilage. Another limitation of this study was the exclusion of a non-seeded HA–co-HDPE material from the cell study. The background assay data from the HA–co-HDPE acellular controls would have further verified the enhanced deposition of mineralized matrix by differentiated BMSCs. The interior of the materials after cell seeding should be examined in the future via cryomicrotoming and subsequent SEM and EDS analysis or histological staining to determine if mineralization occurred within the bulk of the HA–co-HDPE materials. In addition, examination of the effects of varying the molecular weight of HA on the viscoelastic properties and bioactivity should be investigated in the future in order to optimize the HA–co-HDPE for orthopedic applications.

5. Conclusions

HA–co-HDPE is a melt-processable bioactive material, with viscoelastic properties similar to those of articular cartilage, and supports BMSC differentiation and mineralization. HDPE was incorporated to enhance the viscoelastic properties of HA. The results of this study demonstrate that by adjusting the constituent weight ratios in the final composite and incorporating chemical crosslinking, the viscoelastic properties more closely resemble those of articular cartilage. The storage moduli values for HA–co-HDPE show promise for use in replacing articular cartilage. HA–co-HDPE materials have been shown to be non-cytotoxic in their crosslinked and non-crosslinked states, and provide a suitable microenvironment to support mineralization as well as BMSC differentiation into osteoblasts. These findings suggest that HA–co-HDPE holds promise as a permanent implant for the immediate treatment of osteochondral defects that could mimic the dynamic properties of cartilage while permitting osseointegration with the subchondral bone.

Acknowledgements

The authors gratefully acknowledge Dr. Marisha Godek, Ms. Kari Henson and Mr. Drew Henson for their invaluable support in preparing and analyzing cell data, and the Colorado State University Department of Chemistry Central Instrument Facility for the use of instruments. Funding was provided by Schwartz Biomedical, LLC and the Indiana 21st Century Research and Technology Fund.

Appendix A. Figures with essential colour discrimination

Certain figures in this article, particularly Figures 3, 6 and 7, are difficult to interpret in black and white. The full colour images can be found in the on-line version, at doi:10.1016/j.actbio.2010.11.019.

References

[1] Chajra H, Rousseau CF, Cortial D, Ronziere MC, Herbage D, Mallein-Gerin F, et al. Collagen-based biomaterials and cartilage engineering. Application to osteochondral defects. Bio-Med Mater Eng 2008;18:S33–45.
[2] Allison DD, Grande-Allen KJ. Review. Hyaluronan: a powerful tissue engineering tool. Tissue Eng 2006;12(8):2131–40.
[3] Solchaga LA, Goldberg VM, Caplan AI. Hyaluronan and tissue engineering. In: Kennedy JF, Phillips GO, Williams PA, Hascall VC, editors. Hyaluronan. Cambridge: Woodhead; 2000. p. 45–54.
[4] Solchaga LA, Dennis JE, Goldberg VM, Caplan AI. Hyaluronic acid-based polymers as cell carriers for tissue-engineered repair of bone and cartilage. J Orthopaed Res 1999;17:205–13.
[5] Tian WM, Hou SP, Ma J, Zhang CL, Xu QY, Lee IS, et al. Hyaluronic acid-poly-D-lysine-based three-dimensional hydrogel for traumatic brain injury. Tissue Eng 2005;11(3/4):513–25.
[6] Zhao X. Synthesis and characterization of a novel hyaluronic acid hydrogel. J Biomater Sci Polymer Edn 2006;17(4):419–33.
[7] Kogan G, Soltes L, Stern R, Gemeiner P. Hyaluronic acid: a natural biopolymer with a broad range of biomedical and industrial applications. Biotechnol Lett 2007;29(1):17–25.
[8] Noble PW. Hyaluronan and its catabolic products in tissue injury and repair. Matrix Biol 2002;21(1):25–9.
[9] Toole BP. Hyaluronan: from extracellular glue to pericellular cue. Nature Rev Cancer 2004;4(7):528–39.
[10] Aslan M, Simsek Gk, Dayi E. The effect of hyaluronic acid-supplemented bone graft in bone healing: experimental study in rabbits. J Biomater Appl 2006;20:209–20.
[11] Zou L, Zou X, Chen L, Li H, Mygind T, Kassem M, et al. Effect of hyaluronan on osteogenic differentiation of porcine bone marrow stromal cells in vitro. J Orthopaed Res 2008;26(5):713–20.
[12] Chung C, Burdick JA. Influence of three-dimensional hyaluronic acid microenvironments on mesenchymal stem cell chondrogenesis. Tissue Eng: Part A 2009;15(2):243–54.
[13] Hua Q, Knudson CB, Knudson W. Internalization of hyaluronan by chondrocytes occurs via receptor-mediated endocytosis. J Cell Sci 1993;106:365–75.
[14] Bastow ER, Byers S, Golub SB, Clarkin CE, Pitsillides AA, Fosang AJ. Hyaluronan synthesis and degradation in cartilage and bone. Cell Mol Life Sci 2008;65:395–413.
[15] Huang L, Cheng YY, Koo PL, Lee KM, Qin L, Cheng JCY, et al. The effect of hyaluronan on osteoblast proliferation and differentiation in rat calvarial-derived cell cultures. J Biomed Mater Res Part A 2003;66A(4):880–4.
[16] Woodfield TBF, Malda J, de Wijn J, Peters F, Riesle J, Van Blitterswijk CA. Design of porous scaffolds for cartilage tissue engineering using a three-dimensional fiber-deposition technique. Biomaterials 2004;25:4149–61.
[17] Slivka MA, Leatherbury NC, Kieswetter K, Niederauer GG. Porous, resorbable, fiber-reinforced scaffolds tailored for articular cartilage repair. Tissue Eng 2001;7(6):767–80.
[18] Mow VC, Guo XE. Mechano-electrochemical properties of articular cartilage: their inhomogeneities and anisotropies. Ann Rev Biomed Eng 2002;4:172–5.
[19] Collins MN, Birkinshaw C. Physical properties of crosslinked hyaluronic acid hydrogels. J Mater Sci: Mater Med 2008.
[20] Hari PR, Sreenivasan K. Preparation of polyvinyl alcohol hydrogel through the selective complexation of amorphous phase. Journal of Applied Polymer Science 2001;82:143–9.
[21] Noguchi T, Yamamuro T, Oka M, Kumar P, Kotoura Y, Hyon S-H, et al. Poly(vinyl alcohol) hydrogel as an artificial articular cartilage: evaluation of biocompatibility. J Appl Biomater 1991;2:101–7.
[22] Stammen JA, Williams S, Ku DN, Guldberg RE. Mechanical properties of a novel PVA hydrogel in shear and unconfined compression. Biomaterials 2001;22:799–806.
[23] Schmieding R. Inventor. Osteochondral repair using plug fashioned from whole distal femur or condyle formed of hydrogel composition. Washington DC, USA, 2004 2003/08/12/
[24] Oka M. Biomechanics and repair of articular cartilage. J Orthopaed Sci 2001;6:448–56.
[25] Zhang M, James SP. Synthesis and properties of melt-processable hyaluronan esters. J Mater Sci: Mater Med 2005;16:587–93.
[26] Zhang M, James SP. Silylation of hyaluronan to improve hydrophobicity and reactivity for improved processing and derivatization. Polymer 2005;46:3639–48.

[27] Oldinski RA, Cranson CN, James SP. Synthesis and characterization of a hyaluronan-polyethylene copolymer construct for articular cartilage repair. J Biomed Mater Res 2010;94B:441–6.
[28] Saruwatari L, Aita H, Butz F, Nakamura HK, Ouyang J, Yang Y, et al. Osteoblasts generate harder, stiffer, and more delamination-resistant mineralized tissue on titanium than on polystyrene, associated with distinct tissue micro- and ultrastructure. J Bone Miner Res 2005;20(11):2002–2016.
[29] Kessler G, Wolfman M. An automated procedure for the simultaneous determination of calcium and phosphorus. Clin Chem 1964;10:686–703.
[30] Dieudonne SC, van den Dolder J, de Ruijter JE, Paldan H, Peltola T, van 't Hof MA, et al. Osteoblast differentiation of bone marrow stromal cells cultured on silica gel and sol–gel-derived titania. Biomaterials 2002;23(14):3041–51.
[31] Setton LA, Elliot DM, Mow VC. Altered mechanics of cartilage with osteoarthritis: human osteoarthritis and an experimental model of joint degeneration. Osteoarthr Cartil 1999;7:2–14.
[32] Park S, Hung CT, Ateshian GA. Mechanical response of bovine articular cartilage under dynamic unconfined compression loading at physiological stress levels. OsteoArthrit Cartil 2004;12:65–73.
[33] Bueno EM, Bilgen B, Barabino GA. Hydrodynamic parameters modulate biochemical, histological, and mechanical properties of engineered cartilage. Tissue Eng: Part A 2009;15(4):773–85.
[34] Kurkowski RA, Godek ML, Harris JN, James SP. Development of a novel amphiphilic copolymer for biomedical engineering applications. Biomed Eng Soc Ann Fall Meeting, Los Angeles, 2007.
[35] Modder UI, Khosla S. Skeletal stem/osteoprogenitor cells: current concepts, alternate hypothesis, and relationship to the bone remodeling compartment. J Cell Biochem 2008;103:393–400.
[36] Chung C, Beecham M, Mauck RL, Burdick JA. The influence of degradation characteristics of hyaluronic acid hydrogels on *in vitro* neocartilage formation by mesenchymal stem cells. Biomaterials 2009;30:4287–96.
[37] Dadsetan M, Hefferan TE, Szatkowski JP, Mishra PK, Macura SI, Lu L, et al. Effect of hydrogel porosity on marrow stromal cell phenotypic expression. Biomaterials 2008;29:2193–202.
[38] Knudson CB, Knudson W. Hyaluronan-binding proteins in development, tissue homeostasis, and disease. FASEB J 1993;7(13):1233–41.